Analytical Biochemistry 651 (2022) 114697

Contents lists available at ScienceDirect

Analytical Biochemistry

journal homepage: www.elsevier.com/locate/yabio

A novel DNA tweezers-based nanobiosensor for multiple detections of circulating exosomal microRNAs in breast cancer

Melika Agahi, Mahdi Rahaie *

Department of Life Science Engineering, Faculty of New Sciences and Technologies, University of Tehran, Tehran, 14399-57131, Iran

ARTICLE INFO

Keywords:
Biosensor
Multiplex detection
G-quadruplex nanostructure
microRNA
Breast cancer

ABSTRACT

Breast cancer is the prevalent disease in women, and diagnosis of it in early stage and takes preventive measures is very critical. Recently, circulating microRNAs have emerged as promising early biomarkers of cancer. MiR-21 and miR-155 are two significant biomarkers that act as oncomir in breast cancer. In this study, to detect both microRNAs in one test simultaneously, a novel colorimetric nanobiosensor was developed upon the peroxidation property of a specific G-quadruplex nanostructure. The nanostructure forms a DNA Nano-Tweezers after self-assembly of three DNA oligonucleotides with target sequences, and TMB (2, 2′-azino-bis (3-ethylbenzothiazoline-6-sulfonic acid)) is used as a reporter to produce color. The high sensitivity of the nanobiosensor was determined (in buffer and blood) using different concentrations of target sequences with a linear response range from 0 to 10 nM, and detection limit of 0.38 nM ($R^2 = 0.98$). The method precisely detected target sequences from non-target sequences in both buffer and blood media. These findings demonstrate, the nanobiosensor is superior to most previous published works due to its simultaneous dual detection, simplicity, low response time, and cost. The analytical data is convenient for accurately use for clinical purposes to detect breast cancer in early stage, more significantly.

1. Introduction

Cancer occurs due to various factors, such as genetic background, chemical pollution, and unhealthy diet. Breast cancer is the second cause of death in women in the world. It was estimated that in the United States, more than 1.6 million people got cancer, and 700,000 people died of cancer [1–3]. There are several main biomarkers for prognosis and making optimized clinical decision on breast cancer in women including ER (estrogen receptor), PR (progesterone receptor), and HER2 (human epidermal growth factor receptor 2) [4]. Most of the factors involved in the development and progression of breast cancer change the expression of specific regulatory genetic factors, such as microRNAs (miRNAs). MiRNAs can affect tumor genesis or suppression [1–3].

MiRNAs are a class of small, short, non-coding molecules with 18–25 nucleotides long and act as post-transcriptional repressors of gene expression through translational inhibition and/or mRNA destabilization in diverse biological contexts. They could degrade their target mRNAs by hybridizing to 3′-UTR (mostly) [5]. In recent years, various documents have showed that microRNAs are exist from different cells, including cancerous cells, into body fluids such as urine, milk, saliva, and blood, via exosomes (membrane vesicles with a diameter of ~100 nm). Upon the kind of the secreting cells, they embed different molecules including lipids, mRNAs, protein, and miRNAs [6]. Also, it has been shown that miRNAs (circulating exosomal miRNAs) are widely deregulated in human cancers. They play a role in critical development processes [5]; then altered expression of miRNAs could affect the condition and function of the body and cause disease. Thus, circulating exosomal miRNAs can be used as biomarkers to diagnose diseases [7,8]. Hence, design and developing a sensitive, simple, and inexpensive and straightforward method for detecting miRNAs is critical to diagnose cancer in early stages [8–11].

The conventional methods to detect miRNAs such as PCR, RT-qPCR, SplintR-qPCR, require expensive materials, complex design e.x specific primer designing and amplification strategy regards to small size of miRNAs, and complicated procedures such as microRNA extraction for RT reaction from the biological samples or application of chlorella virus DNA ligase which are not suitable for a simple practical approach [12]. Thus, introducing the simple and feasible and straightforward ways such as colorimetric DNA-based biosensors with naked-eye recognition is ideal for convenient microRNA and nucleic acid detection. In this way, a

* Corresponding author.
E-mail address: mrahaie@ut.ac.ir (M. Rahaie).

https://doi.org/10.1016/j.ab.2022.114697
Received 21 February 2022; Received in revised form 4 April 2022; Accepted 24 April 2022
Available online 26 April 2022

signal must be generated when only the target is identified. DNA and RNA can take many different forms. G-quadruplex is a secondary structure of DNA that is non-canonical and has G-rich sequences. Gq consists of four guanines, which are held together by Hoogsteen hydrogen bonds. The particular structure plays a vital role *in vivo*, such as telomere maintenance [13], transcription, and DNA replication [14,15], malignant transformation and cancer development [16,17]. The formation of G-quadruplex can create instability in genome by inducing mutations (including deletions), and stimulating recombination events. The significant role of the structures in the characterization of malignant cells has already been found in breast cancer specimens [18,19]. Because of the functions that G4s have *in vivo*, many researchers have developed G4-based sensors [20,21]. Also, G-quadruplex, with hemin (as a co-factor) shows a catalytic activity into specific hydrogen peroxide mediated oxidation substrates, such as ABTS2 (2, 20-azino-bis (3-ethylbenzthiazoline-6-sulfonic acid), TMB, and *o*-phenylenediamine [22–25].

In this work, it was fabricated a colorimetric biosensor upon utilizing a split G-quadruplex (Gq) nanostructure and its peroxidase-mimicking property to detect simultaneous dual detections of two circulating microRNAs (miR-21 and miR-155).

2. Experimental

2.1. Regents

NH_4Cl, KCl, Tris-HCl, Triton-X100, H_2O_2 solution (30%), Tetramethylbenzidine (TMB), Dimethyl sulfoxide (DMSO), and Hemin were obtained from Sigma (USA) and Merck (Germany) in analytical grade. DNA oligonucleotides were purchased from Metabion Company (Germany). Deionized water was used for the preparation of all solutions.

2.2. Production of DNA Nanotweezers (DNA-NT)

All used oligonucleotides are listed in Table 1. Unafold software (http://www.unafold.org/mfold/applications/dna-folding-form.php) was used to confirm secondary structure of oligos, *in silico*. Each oligonucleotide was solved in phosphate buffer saline to be 5 μM and then was kept at 95 °C for 5 min. Then it was slowly cooled to room temperature (RT) to form the DNA-NanoTweezers by a self-assembly process. Agarose gel electrophoresis was used to confirm the nanostructure formation. The resultant was stored at 4 °C until use.

2.3. Catalytic reaction

To provide 10 mM of Hemin and 100 μM of TMB solutions, they solved into DMSO, separately. The DNA-NanoTweezers oligos (50 nM) with 50 nM of each target sequences (miRNA-21, miRNA-155), and hemin (2 μM final) were mixed in 178 μL of a specific working buffer ((150 mM NH_4Cl, 20 mM KCl, 50 mM Tris–HCl, and TritonX-100 0.03%) (pH 7.5)) in a 2 mL vial, and kept for 1 h at room temperature. Then 2 μl of TMB (10 mM) was added to the solution and after the addition of 20 μL of H_2O_2 (10 mM) to it, the 650 nm spectrum was selected to record absorbance ratio of the solution.

Table 1
The oligonucleotides sequences. Complementary regions are shown in similar color.

Name	5′ 3′
O1	GGGTTGGGTTTATAGGATGTCGGAGGCATTAGGACTTTTGGGTAGGG
O2	CCGACATCCTATTCAACATCAGAACCCCTATCAC
O3	CCGTAATCCTGAATCGAATAGTCAATTACGATTAG
miR-21-5p	TAGCTTATCAGACTGATGTTGA
miR-155-5p	TTAATGCTAATCGTGATAGGGGTT

2.4. The sensitivity assay, linearity response range, and LOD

First, 100 μl of DNA-NT oligos (50 nM), and 10 μl of each target sequences (miR-21 and miR-155) at different concentrations (2, 4, 6, 8, and 10 nM) along with 2 μl of hemin (100 μM), as the co-factor of Gq structure, were dissolved in 178 μl of the above mentioned working buffer. Then, they were incubated at room temperature for 1 h. After this, 2 μl of TMB (10 mM) and 20 μl of H_2O_2 (10 mM) were added. The solution was measured (in three replicates) for absorption spectra ratio (with a Nanodrop 2000C, Thermoscientific, USA).

Limit of detection (LOD) was calculated upon the formula ($LOD = \frac{F*SD}{b}$), in which SD is the standard deviation of the absorbance ratio of blank sample in the 650 nm spectrum, b is the slope of the regression line and F is equal to 3.3.

2.5. The specificity assessment

To determine the selectivity of the nanobiosensor, specificity experiments were performed by using non-target sequences and without/with of target sequences. Concentration of 50 nM of each target and non-target sequences were added to the reaction solution (mentioned working buffer in section 2.3). The absorption ratio was measured for one target sequence, as well. All measurements were done with a Nanodrop 2000C spectrophotometer (Thermoscientific, USA).

2.6. Detection of target miRNAs in the real sample

2.6.1. The sensitivity assay

To evaluate the sensitivity of nanobiosensor in the real sample, it was assessed in blood plasma. The plasma was isolated from the blood taken from a healthy woman aged 33 years following relevant and approved guidelines and collected in a tube containing EDTA. The samples were centrifuged at 150*g for 5 min (two times) and then 350*g for 15 min at room temperature, and in follow, the plasma was collected and kept at −20 °C until use. It was diluted with reaction buffer (refer to section 2.3 with ratio of 1:50 plasma/buffer). In 2 mL vials, four concentrations of target miRNAs (0, 10, 20, 40 nM) were added (in three replicates) to the diluted plasma. All absorbance measurements were done with a Nanodrop 2000C spectrophotometer (Thermoscientific, USA).

2.6.2. The specificity test

To evaluate the specificity of the nanobiosensor in the real sample, diluted blood plasma (refer to section 2.6.1) was used as a reaction medium. As mentioned above, after isolation of plasma and dilution, 50 nM of each non-target sequences were added to the plasma along with the target sequences. Also, the absorption spectra was measured for one target.

3. Results and discussions

3.1. Principles for detection with the nanobiosensor

Scheme 1 shows the principle of dual detections in our work. It was used a DNA-NT nanostructure to detect double target microRNAs. Each split Gq sequence has two recognition sites (reverse complement) for complementary sequences of target microRNAs. The split Gqs were closed to each other due to the hybridization of the target recognition sites with the target microRNAs. In other words, when target sequences bind to these split Gqs, they change the split G quadruple from an open state to a complete and closed state form which has a peroxidase-like activity. Five oligos are used in the method; two targets (miRNAs), and three probe sequences, to form a nanostructure for the production of a peroxidase-like activity. This enzymatic activity was assayed by TMB oxidation, which produces a blue color for naked-eye observation. MicroRNA-21 and microRNA-155 were selected as the targets due to

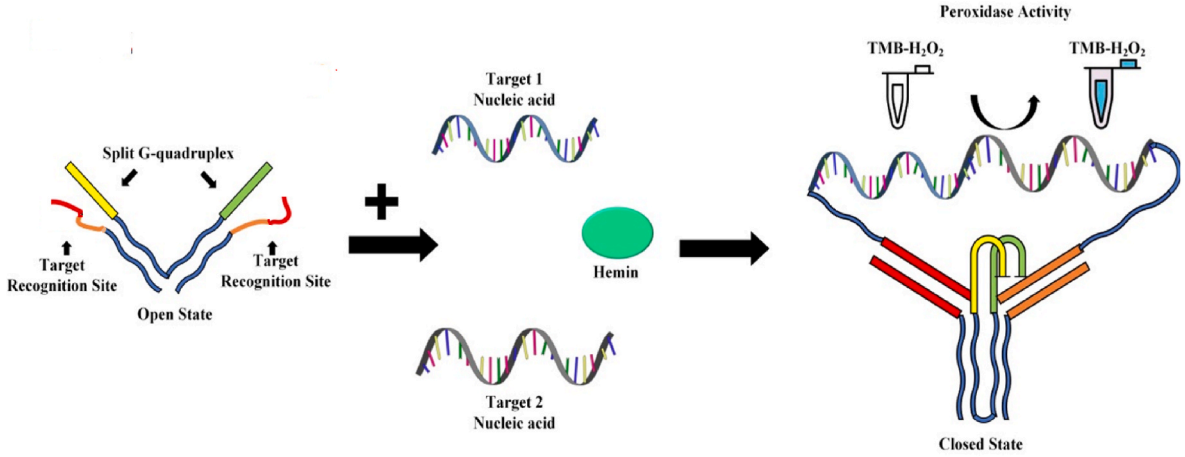

Scheme 1. The principle of the nanobiosensor. Each split Gq sequence (open state) has two recognition sites (reverse complement) for a complementary sequences of target microRNAs (miR-21 and miR-155).

their significant role as oncomirs in breast cancer.

The peroxidase mimic catalytic reaction as of any other oxidor-eduction reaction, consists of two halves 1- oxidation of a reductant (TMB) and 2- reduction of an oxidant (H_2O_2). DNA-NT-Hemin structure acts as a catalyst to oxidize TMB and then color change. Hemin (as a weak oxidizer for TMB) cant solely cause to TMB oxidation [26,27].

3.2. The optimization of nanobiosensor parameters

To obtain more stable and optically distinguished spectra, it was adjusted the reaction conditions of the nanobiosensor, and the effect of different parameters including, concentrations of H_2O_2 (0–50 mM) and TMB (0–16 mM) on the nanobiosensor performance was investigated.

As shown in Fig. 1, by increasing H_2O_2 concentration, the rate of absorption increases. Different concentrations of TMB also affect absorption ratio. Fig. 2, shows that absorption rate is enhanced with increasing TMB concentration.

It seems with increasing the concentration of H_2O_2 (Fig. 1), the DNAzyme (G4+Hemin) peroxidase mimic catalytic activity reduced slowly to a steady level. It may be due to decrease the pH of reaction buffer in presence of more concentration of H_2O_2. As a result, it structure is disrupted and it catalytic activity is eliminated or stopped, and then, TMB is oxidized as long as DNA-NT-Hemin is maintained. In the work done by Li et al. It was found the DNAzyme/hemin had the maximum catalytic activity when amount of H_2O_2 increased by five times of TMB not more [28]. Due to get the highest absorption spectrum (Figs. 1, and Fig.2), the concentration of 10 mM of each H_2O_2 and TMB, as optimized concentration of the parameters, was used for main analysis related to nanobiosensor.

In order to optimize the hybridization time, the absorption ratio of the HCR reaction at three different times were measured. As shown in Fig. 3, there is no difference among various hybridization times, then a time of 1 h as at least required time, was considered for hybridization of oligos and target miRNAs sequences.

3.3. Assessment of G4 formation and peroxidase activity induced by microRNAs

After hybridization of the target sequences (miRNAs), the split Gq-based nanostructure changes its structure from open to a closed state. As split Gqs get closer to each other, the distance between them decreases and restores enzymatic activity. Electrophoresis was used to confirm the formation of the G-quadruplex structure (Fig. 4a). The self-aggregation of three oligonucleotides (O1, O2, and O3, Table 1) results in the formation of open Gq-based DNA-NT. O1 acts as a base for the hybridizing O2 and O3. Two oligonucleotides (O2, O3) have a target recognition site for hybridization with microRNAs. Regards to the sequences of O2 and O3 (Table 1), they can only hybridize to miR-21 and miR-155, not every other microRNAs or more than two microRNAs and the closed Gq-based DNA-NT is constructed just in the presence of the targets. Therefore this engineered nanostructure guarantees specific double detection of the target microRNAs. The position of each band on the gel was compared to confirm the successful structure. All oligonucleotides are almost in the same position because there is not much difference in the number of nucleotides. In the fourth well, O1 + O2 + O3 was observed to be in an upper position and more intensity than others due to having more closed shape. As it can't be recognized hybridization process of target sequences to Gq oligos with electrophoresis in our work (due to specific design, there is no difference in position of bands on gel in the presence/absence of target sequences), then, to assess peroxidase activity of the DNA-NT nanostructure and confirmation of both targets hybridization, the TMB oxidizing reaction was

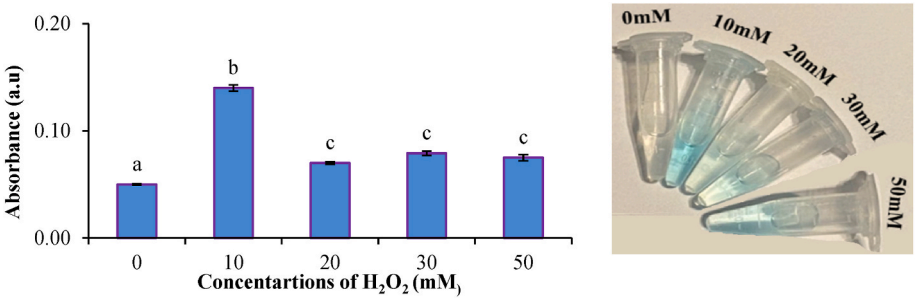

Fig. 1. Different concentrations of H_2O_2 (from 0 to 50 mM) at a constant concentration of TMB (10 mM) in the presence of DNA-NT structure (50 nM). Error bares (repeatability) show standard error (SE) with three replications ($P < 0.05$).

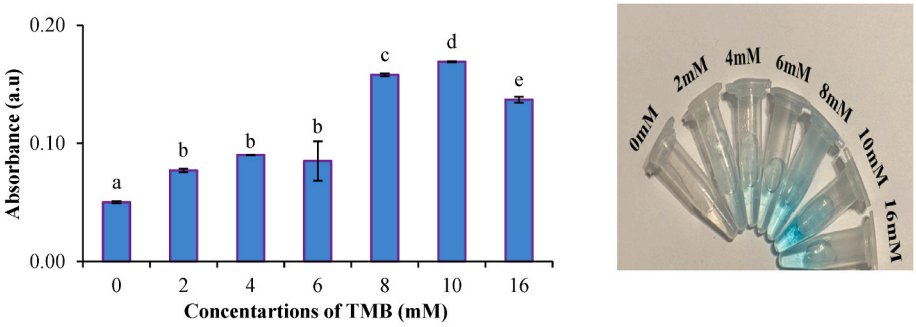

Fig. 2. Different concentrations of TMB (from 0 to 16 mM) with a constant concentartion of H_2O_2 (10 mM) in the presence of DNA-NT structure (50 nM). Error bares (repeatability) show standard error (SE) with three replications ($P < 0.05$).

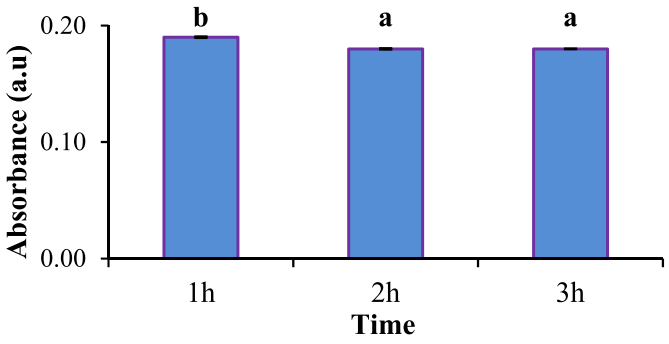

Fig. 3. The effect of hybridization time on absorption ratio. Error bares (repeatability) show standard error (SE) with three replications ($P < 0.05$).

assayed which exhibits colorimetric absorbance at 650 nM, and it can be seen with the naked eye (Fig. 4b).

3.4. The sensitivity assessment

To measure the sensitivity of the nanobiosensor, different concentrations of target sequences (miR-21 and miR-155) were used. Change the concentration alters the observed color intensity. With increasing concentration of the target sequences from 2 nM to 10 nM, the color intensity (the absorption rate in the 650 nm) also increases (Fig. 5). The linearity response range for the nanobiosensor was obtained from 0 to 10 nM ($R^2 = 0.98$) with a limit of detection of 0.38 nM. Regards to low concentration range of circulating microRNAs in blood (fM-nM) [24] and the obtained LOD (0.38 nM), it seems that the method has a high precision for detecting microRNAs involved in breast cancer by a simple and inexpensive colorimetric method that can be used in clinical diagnoses. Although miR-21 and miR-155 in breast cancer patients' blood have different expression levels but in various reports [29–31], it has been found that their upregulation is directly positively correlated to each other and both are increased significantly. Therefore, it seems that the present biosensor has the competence to use for simultaneous detection of these microRNAs. Table 2 shows the brief results of several published reports about multiple or dual detections of different significant biomarkers. The comparison between the table data and our work shows the superiority and innovating the present biosensor for introducing a novel and simple colorimetric method with nearly high sensitivity for multi-detection of breast cancer biomarkers with a significant LOD.

3.5. The specification measurement

To measure the specification of nanobiosensor, it was used non-target microRNAs (microRNA-137, microRNA-193). As shown in Fig. 6, the absorption ratio in the presence of target sequences was compared with when there were no sequences or non-target sequences. It was proved that this nanobiosensor has a high specificity to identify the target sequences. As shown in Fig. 6, absorption rate is also measured with one target (miR-21), which has lower absorption compared to two target sequences. It was confirmed the method could recognize the dual microRNAs from others well. In clinical assays, diagnosis of a disease can increase with unique detection of a specific biomarker and also increasing the number of analyzed biomarkers in one test.

3.6. The sensitivity and selectivity assays in the real sample (blood)

Due to the importance of detecting breast cancer in the early stage and to prove the feasibility of our method utility for the evaluation of clinical samples, we recognized miR-21 and miR-155 in human blood

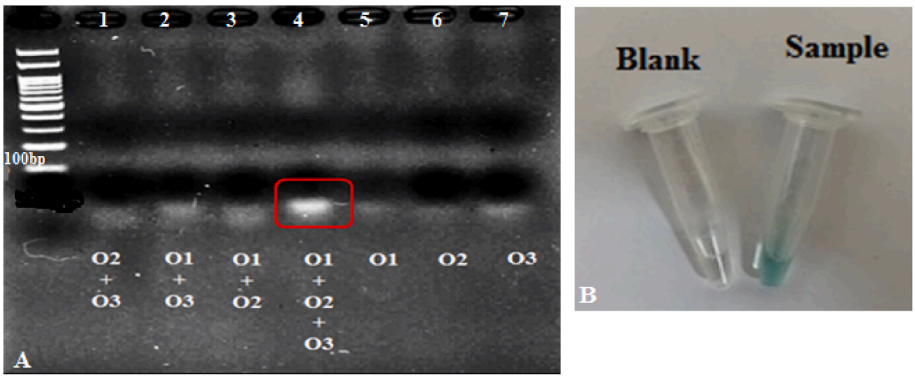

Fig. 4. The confirmation of G-quadruplex formation by electrophoresis (a). O1, 2, 3 are sequences 1–3 in Table 1. The assessment of peroxidation property of G-quadruplex (b). Blank is Gq without H_2O_2 and TMB, and the Sample is Gq with H_2O_2 and TMB.

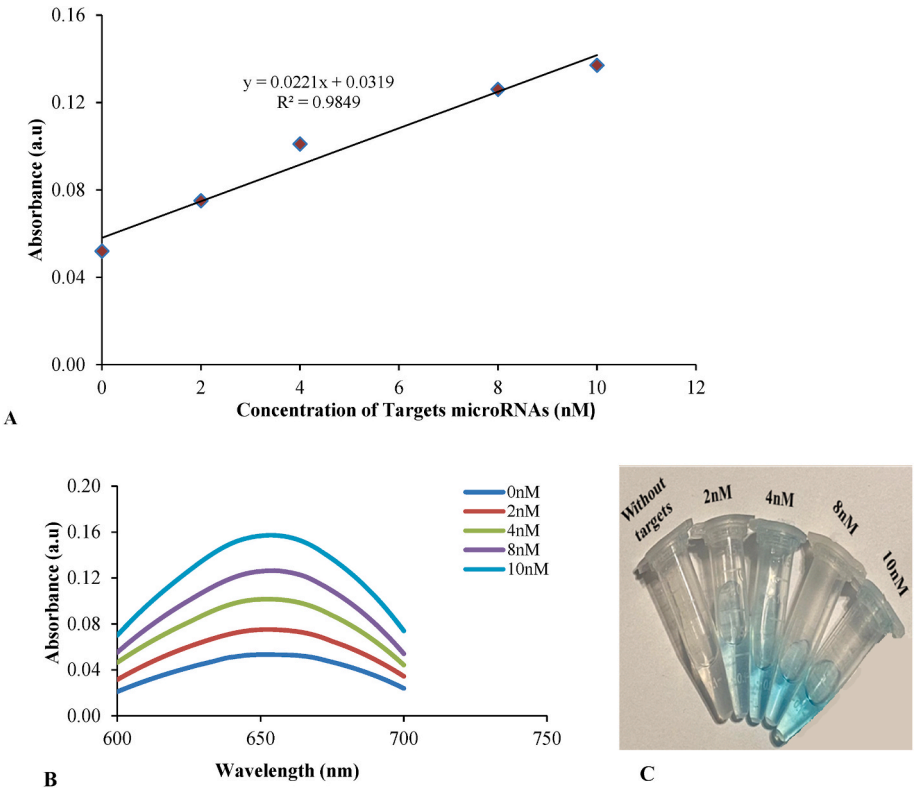

Fig. 5. A) The linearity range of the nanobiosensor within 0–10 nM of target microRNAs. Each point was replicated for 3 times, but due to low standard error, the error bar can't be seen in the diagram. b) The enhancement of absorption spectrum with increasing concentration of targets and c) color intensity with increasing targets concentrations. (For interpretation of the references to color in this figure legend, the reader is referred to the Web version of this article.)

Table 2
The comparison among published biosensors related to multi detection of different biomarkers.

No	Number of analytes	Method	Linear range	LOD	Ref.
1	2	Colorimetric	2 nM–10 nM	0.38 nM	This work
2	2	electrochemical	0.1 fM to 10 nM	miRNA-21:18.9 aM miRNA-155:39.6 aM	[32]
3	2	Fluorescence	0.5 nM–5 nM	82pM	[24]
4	2	electrochemical	1 fM to 1 μM	miR-1246: 0.19 fM miR-4521:0.28 fM	[25]
5	3	SERS	–	sPD-1:6.17 pg/mL sPD-L1:0.68 sEGFR:69.86	[18]
6	2	Spectroscopy	10 nM–100 nM	AFP:2.4 nM CEA:5.6 nM	[12]
7	2	Electrochemical immunoassay	10^{-6}-1U/mL 10^{-4}-100 U/mL	CA125:0.1μU/mL CA15–3:10 μU/mL	[5]
8	2	Microfluidic system	1–40 ng/mL	CEA:0.3 ng/mL PSA:0.4 ng/mL	[33]

plasma samples. The results (Fig. 7) showed that this nanobiosensor could be applied in the real sample; but the sensitivity of nanobiosensor (LOD = 1.6 nM with a linearity response range of 0–40 nM) was reduced presumably due to interference with blood proteins and other biomolecules. It is appeared the biosensor sensitivity is reduced by ~1/4 compared with into buffer. However, as mentioned before, due to the usual concentration of these miRNAs in blood (fM-nM), the nanobiosensor, even with the LOD (1.6 nM) can be used for monitoring of the biomarkers in clinical cancer samples.

To assess the selectivity of our method in a real sample, it was detected target sequences alongside non-target sequences in human plasma samples. As shown in Fig. 8, the results showed that this nanobiosensor could distinguish the target sequences from the non-target sequence in the blood.

4. Conclusions

Diagnosis of breast cancer in early stages can help the effective treatment of the disease in patients. It has been found that MicroRNAs act as an early biomarkers for cancer detection. In this work, we have designed and fabricated a nanobiosensor based on a split G-quadruplex based DNA-Nano Tweezers for detecting dual microRNA biomarkers. The nanostructure with peroxidase activity specifically identified the miR-21 and miR-155 as significant biomarkers involved in breast cancer. A LOD of 0.38 nM with a linearity range of 0–10 nM ($R^2 = 0.98$) of target microRNAs in buffer and high selectivity in buffer and blood media were obtained. This biosensor proved superior to most previous published works due to its simultaneous dual detection, simplicity, low response time, and cost. The analytical data of this study in the real sample (blood) can be used for the clinical purposes to detect breast cancer in the early stage, more significantly.

Competing interests

The authors state that there is no conflict of interest in publishing this article.

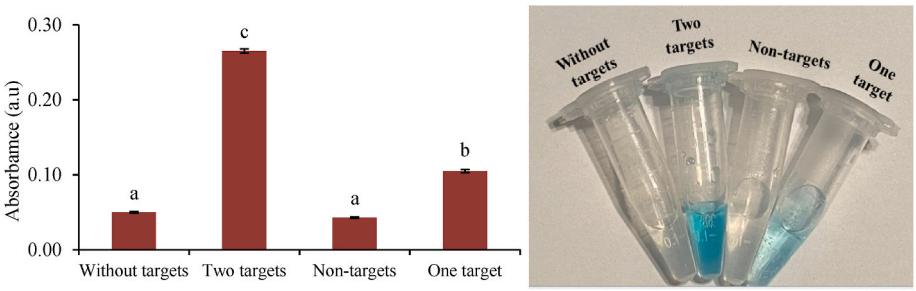

Fig. 6. Left) The selectivity of nanobiosensor with 50 nM of targets, non-targets, and one target microRNA (miR-21). Right) Different color intensity in 650 nm. Error bares (repeatability) show standard error (SE) with three replications ($P < 0.05$). (For interpretation of the references to color in this figure legend, the reader is referred to the Web version of this article.)

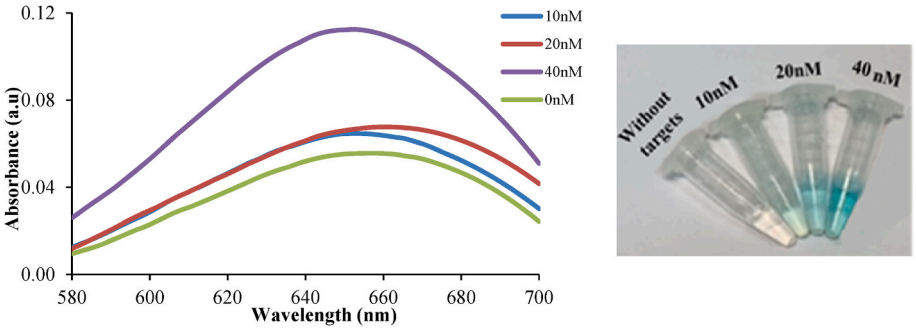

Fig. 7. Increase of the absorption ratio and color intensity with increasing target microRNAs concentrations in blood plasma. (For interpretation of the references to color in this figure legend, the reader is referred to the Web version of this article.)

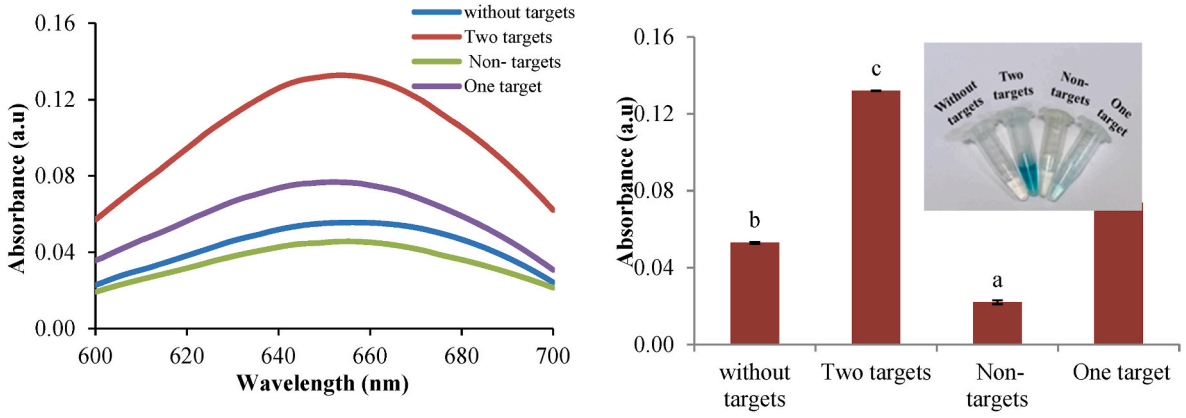

Fig. 8. The selectivity examination with 50 nM of targets, non-targets, and one target microRNA (miR-21) in plasma medium. It shows different absorbance spectra in 650 nm and color intensity. Error bares (repeatability) show standard error (SE) with three replications ($P < 0.05$). (For interpretation of the references to color in this figure legend, the reader is referred to the Web version of this article.)

Funding

This work was supported by University of Tehran.

Authors' contributions

Both authors contributed to the study conception and design. Material preparation, data collection and experimental works were performed by M. Agahi and M. Rahaie. The initial draft of the manuscript was written by M. Agahi and M. Rahaie commented on previous versions of the manuscript. Both authors read and approved the final manuscript.

Declaration of competing interest

None.

Acknowledgement

The authors acknowledge the instrumental support of University of Tehran.

References

[1] M. Abolghasemi, S.S. Tehrani, T. Yousefi, A. Karimian, A. Mahmoodpoor, A. Ghamari, F. Jadidi-Niaragh, M. Yousefi, H.S. Kafil, M. Bastami, MicroRNAs in breast cancer: roles, functions, and mechanism of actions, J. Cell. Physiol. 235 (2020) 5008–5029.

[2] Z. Ali Syeda, S.S.S. Langden, C. Munkhzul, M. Lee, S.J. Song, Regulatory mechanism of microRNA expression in cancer, Int. J. Mol. Sci. 21 (2020) 1723.
[3] M.Y. Alzahrani, A. Alahmadi, Breast cancer image classification using the convolution neural network, Int. J. Adv. Trends Comput. Sci. Eng. 8 (2019) 3447–3453.
[4] P. Gamble, R. Jaroensri, H. Wang, F. Tan, M. Moran, T. Brown, I. Flament-Auvigne, E.A. Rakha, M. Toss, D.J. Dabbs, Determining breast cancer biomarker status and associated morphological features using deep learning, Commun. Med. 1 (2021) 1–12.
[5] B. Babamiri, R. Hallaj, A. Salimi, Ultrasensitive electrochemiluminescence immunoassay for simultaneous determination of CA125 and CA15-3 tumor markers based on PAMAM-sulfanilic acid-Ru (bpy) 32+ and PAMAM-CdTe@ CdS nanocomposite, Biosens. Bioelectron. 99 (2018) 353–360.
[6] H. Ogata-Kawata, M. Izumiya, D. Kurioka, Y. Honma, Y. Yamada, K. Furuta, T. Gunji, H. Ohta, H. Okamoto, H. Sonoda, Circulating exosomal microRNAs as biomarkers of colon cancer, PLoS One 9 (2014), e92921.
[7] T.M. Bryan, Mechanisms of DNA replication and repair: insights from the study of G-quadruplexes, Molecules 24 (2019) 3439.
[8] J. Carvalho, J.-L. Mergny, G.F. Salgado, J.A. Queiroz, C. Cruz, G-quadruplex, friend or foe: the role of the G-quartet in anticancer strategies, Trends Mol. Med. 26 (2020) 848–861.
[9] J. Chen, R. Zhou, Y. Liang, X. Fu, D. Wang, C. Wang, Blockade of lncRNA-ASLNCS5088–enriched exosome generation in M2 macrophages by GW4869 dampens the effect of M2 macrophages on orchestrating fibroblast activation, Faseb. J. 33 (2019) 12200–12212.
[10] P.J. Dexheimer, L. Cochella, MicroRNAs: from mechanism to organism, Front. Cell Dev. Biol. 8 (2020) 409.
[11] Y. Guo, W. Yao, R. Pei, Label-free Biosensors for Early Diagnosis of Cancer Based on G-Quadruplex and Isothermal Amplification, Next Generation Point-of-care Biomedical Sensors Technologies for Cancer Diagnosis, Springer, 2017, pp. 83–114.
[12] Y. Jiang, Y. Tang, P. Miao, Polydopamine nanosphere@ silver nanoclusters for fluorescence detection of multiplex tumor markers, Nanoscale 11 (2019) 8119–8123.
[13] T. Kilic, A. Erdem, M. Ozsoz, S. Carrara, microRNA biosensors: opportunities and challenges among conventional and commercially available techniques, Biosens. Bioelectron. 99 (2018) 525–546.
[14] N. Kosiol, S. Juranek, P. Brossart, A. Heine, K. Paeschke, G-quadruplexes, A promising target for cancer therapy, Mol. Cancer 20 (2021) 1–18.
[15] I. Krepelkova, T. Mrackova, J. Izakova, B. Dvorakova, L. Chalupova, R. Mikulik, O. Slaby, M. Bartos, V. Ruzicka, Evaluation of miRNA detection methods for the analytical characteristic necessary for clinical utilization, Biotechniques 66 (2019) 277–284.
[16] L. Lan, R.-L. Wang, L. Liu, L. Cheng, A label-free colorimetric detection of microRNA via G-quadruplex-based signal quenching strategy, Anal. Chim. Acta 1079 (2019) 207–211.
[17] L.K. Lerner, J.E. Sale, Replication of G quadruplex DNA, Genes 10 (2019) 95.
[18] J. Li, J. Wang, Y.S. Grewal, C.B. Howard, L.J. Raftery, S. Mahler, Y. Wang, M. Trau, Multiplexed SERS detection of soluble cancer protein biomarkers with gold–silver alloy nanoboxes and nanoyeast single-chain variable fragments, Anal. Chem. 90 (2018) 10377–10384.
[19] A. Moridikia, H. Mirzaei, A. Sahebkar, J. Salimian, MicroRNAs: potential candidates for diagnosis and treatment of colorectal cancer, J. Cell. Physiol. 233 (2018) 901–913.
[20] M.H. Choi, Y.J. Seo, Rapid and highly sensitive hairpin structure-mediated colorimetric detection of miRNA, Anal. Chim. Acta 1176 (2021) 338765.
[21] J. Ge, Z. Qi, L. Zhang, X. Shen, Y. Shen, W. Wang, Z. Li, Label-free and enzyme-free detection of microRNA based on a hybridization chain reaction with hemin/G-quadruplex enzymatic catalysis-induced MoS 2 quantum dots via the inner filter effect, Nanoscale 12 (2020) 808–814.
[22] K. Nakatsuka, H. Shigeto, A. Kuroda, H. Funabashi, A split G-quadruplex-based DNA nano-tweezers structure as a signal-transducing molecule for the homogeneous detection of specific nucleic acids, Biosens. Bioelectron. 74 (2015) 222–226.
[23] M. Nishio, K. Tsukakoshi, K. Ikebukuro, G.- quadruplex, Flexible conformational changes by cations, pH, crowding and its applications to biosensing, Biosens. Bioelectron. (2021) 113030.
[24] M. Rahaie, S.K. Noroozi, A nanobiosensor based on graphene oxide and DNA binding dye for multi-microRNAs detection, Biosci. Rep. 39 (2019), BSR20181404.
[25] H. Rezaei, M. Motovali-Bashi, S. Radfar, An enzyme-free electrochemical biosensor for simultaneous detection of two hemophilia A biomarkers: combining target recycling with quantum dots-encapsulated metal-organic frameworks for signal amplification, Anal. Chim. Acta 1092 (2019) 66–74.
[26] E. Ruggiero, S.N. Richter, G-quadruplexes and G-quadruplex ligands: targets and tools in antiviral therapy, Nucleic Acids Res. 46 (2018) 3270–3283.
[27] M.M.H. Sohel, Circulating microRNAs as biomarkers in cancer diagnosis, Life Sci. 248 (2020) 117473.
[28] J. Tan, L. Lan, The DNA secondary structures at telomeres and genome instability, Cell Biosci. 10 (2020) 1–6.
[29] M.M. Itani, F.J. Nassar, A.H. Tfayli, R.S. Talhouk, G.K. Chamandi, A.R.S. Itani, J. Makoukji, R.-M.N. Boustany, L. Hou, N.K. Zgheib, A Signature of four circulating microrna as potential biomarkers for diagnosing early-stage breast cancer, Int. J. Mol. Sci. 22 (2021) 6121.
[30] J.-G. Han, Y.-D. Jiang, C.-H. Zhang, Y.-M. Yang, D. Pang, Y.-N. Song, G.-Q. Zhang, A novel panel of serum miR-21/miR-155/miR-365 as a potential diagnostic biomarker for breast cancer, Annals of surgical treatment and research 92 (2017) 55–66.
[31] S. Farsinejad, M. Rahaie, A.M. Alizadeh, M. Mir-Derikvand, Z. Gheisary, H. Nosrati, S. Khalighfard, Expression of the circulating and the tissue microRNAs after surgery, chemotherapy, and radiotherapy in mice mammary tumor, Tumor Biol. 37 (2016) 14225–14234.
[32] S. Xu, Y. Chang, Z. Wu, Y. Li, R. Yuan, Y. Chai, One DNA circle capture probe with multiple target recognition domains for simultaneous electrochemical detection of miRNA-21 and miRNA-155, Biosens. Bioelectron. 149 (2020) 111848.
[33] Y. Wang, Y. Xia, Optical, electrochemical and catalytic methods for in-vitro diagnosis using carbonaceous nanoparticles: a review, Microchim. Acta 186 (2019) 50.